

Received November 22, 2021, accepted December 5, 2021, date of publication December 8, 2021, date of current version December 21, 2021.

Digital Object Identifier 10.1109/ACCESS.2021.3133886

# Laser-Induced Breakdown Spectroscopy-Based Coal-Rock Recognition: An *in Situ* Sampling and Recognition Method

CONG LIU<sup>1</sup>, YIMIN LUO<sup>1,2</sup>, AND QIZHI ZHANG<sup>1</sup>

<sup>1</sup>China Coal Technology and Engineering Group Shanghai Company Ltd., Shanghai 200040, China

<sup>2</sup>State Key Laboratory of Advanced Optical Communication Systems and Networks, Shanghai Jiao Tong University, Shanghai 200000, China

Corresponding author: Cong Liu (liucong@alumni.sjtu.edu.cn)

This work was supported in part by the National Basic Research Program of China under Grant 2014CB046306.

**ABSTRACT** Coal and rock recognition (CRR) has important theoretical and practical significance in unmanned coal mining. Laser-induced breakdown spectroscopy (LIBS) is considered a cutting-edge technology in the field of material analysis due to its real-time analysis capability, minimal to no sample preparation scheme, high sensitivity to low atomic weight elements, and ability to perform nearby and distant detection. In this research, a new fast and accurate coal-rock recognition method for unmanned coal mining based on LIBS is presented. The LIBS *in situ* sampling method of the coal mining face and the LIBS-based CRR method are discussed. Partial least squares discriminant analysis (PLS-DA) is used to analyze the LIBS spectrum and to construct a simplified spectral model (SSM). Finally, SSM and neural network classifiers are used to recognize coal and rock, and the results are presented and discussed. These results show that the CRR method proposed in this research has a high recognition accuracy rate.

**INDEX TERMS** Coal-rock recognition (CRR), laser-induced breakdown spectroscopy (LIBS), *in situ*, unmanned coal mining.

## I. INTRODUCTION

There is an urgent need for an effective method for unmanned working faces in coal mines to achieve safety, efficiency, and intelligent mining. The key basic problem restricting the intelligent mining of underground coal mines is the intelligent and precise perception of the mining environment. Coal-rock recognition (CRR) is one of the key technologies for realizing unmanned working faces; CRR is also the core technology for realizing intelligent and precise perceptions of mining environments. However, CRR has always been a major unsolved problem related to the research and application of unmanned and intelligent mining in coal mines [1], [2].

The recognition rate is crucial for CRR. A high-recognition CRR plays a key role in helping picks avoid rocks in time, greatly reducing the possibility of gas explosions caused by the dangerous temperatures generated by picks cutting rocks [3], [4]. In addition, CRR also realizes the rapid separation of coal gangue in coal preparation plants.

The associate editor coordinating the review of this manuscript and approving it for publication was Qiuye Sun<sup>1</sup>.

To date, considerable research has been devoted to various CRR methods, including the cutting force monitoring method, detection method, vibration detection method, acoustic detection method,  $\gamma$ -ray detection method, radar detection method, and image analysis method [5]–[11].

In fact, these methods have certain dependences on the geological conditions and coal mining technologies. Likewise, it is difficult to popularize and apply such methods to actual production because of their small application scope and low recognition accuracy.

Considering the status of current research, a good analysis performance CRR technique is significant and necessary. The characteristic difference of coal and rock material composition has the advantages of not relying on specific conditions and not being easily disturbed by the environment. In the future, effective active coal and rock identification technology will use *in situ* material analysis technology to identify coal and rock based on the material composition.

At present, there are few material analysis methods that are suitable for CRR.

A variety of online analysis methods with *in situ*, online and real-time detection capabilities are applied in industrial

engineering, such as X-ray fluorescence (XRF) [12], prompt gamma neutron activation analysis (PGNAA) [13], [14], and near-infrared spectrometry (NIRS) [15].

XRF and PGNAA are relatively ideal material analysis techniques. These techniques use different rays to analyze and identify the elements and corresponding concentrations that are present in materials, and they have achieved good practical results in some industrial applications. However, the corresponding detection equipment is very heavy (the minimum weight of the machine with PGNAA technology is 3200 kg [16]), which is not suitable for crowded coal mining face environments, and the radioactive sources used have potential health hazards. The use of such equipment is strictly controlled based on regulatory restrictions.

In addition, most material analysis technologies, including XRF and PGNAA technologies, do not have high analysis accuracies for low atomic number elements such as carbon (C) and silicon (Si), so they cannot satisfactorily meet the needs of coal and rock identification.

In this research, a new idea for coal-rock recognition in unmanned coal mining based on laser-induced breakdown spectroscopy (LIBS) is presented.

LIBS is considered a front runner in chemical analysis due to its unique features, such as real-time analysis, pseudo nondestructive techniques, minimal to no sample-preparation protocols, a high sensitivity to low atomic weight elements, and a capability to carry out close-up and far-away detection.

As a consequence, over the last two decades, LIBS has been widely applied in a variety of fields, such as environmental monitoring [17], [18], biomedical applications [19], [20], archeological investigations [21], [22], pharmaceutical applications [23], [24], extraterrestrial explorations [25]–[28], hazardous materials identification [29], nuclear fuel characterization [30], [31], and geological material characterization [26], [32], [33]. In addition, LIBS has also been used to detect insulation failures in the power supplies used in medium voltage applications [34]. Several laser-based methods have been recently developed to analyze coal-rock [35]–[38]. In such methods, each plasma radiation spectral line corresponds to unique transitions in the atoms, ions, or molecules. These are used as “fingerprints” to identify the sample structure [39]. Therefore, LIBS can be used to classify and recognize different substances. The advantages of LIBS include the nondestructive assessment of small samples, fast detection, no initial preparation requirement, no radioactive source requirement, and online and in situ analysis capabilities [40], [41].

Dr. He [42] presented research on the gas explosion mechanism, which is in accordance with the free radical mechanism of the vapor reaction and the spectral theory of polyatomic molecules. As long as the laser pulse energy intensity is strictly controlled, the safety laser instrument use in the coal mining working face can be guaranteed. Hai obtained safe laser application conditions in coal mines, providing theoretical support for LIBS application to coal mine working faces. In addition, the application of multivariate chemometric

methods in conjunction with LIBS data has recently shown tremendous potential in the field of coal analysis. LIBS uses chemometric methods — linear or parametric correlation, principal component analysis [43], partial least-squares analysis [44], [45], etc. — to identify organic compounds. All of these results show that the use of LIBS for CRR is very promising.

The LIBS-based coal-rock recognition (LIBS-CRR) method uses advanced material analysis technology to identify coal and rock according to the material composition. This method has the advantages of not being dependent on specific conditions and not being susceptible to environmental interference. In addition, LIBS technology has many advantages, such as no required sample preparation and in situ, rapid and multielement simultaneous detection, and there is no radiation risk of X-ray and  $\gamma$ -ray material analysis technology. LIBS can effectively detect carbon (C), nitrogen (N), oxygen (O), magnesium (Mg), aluminum (Al), silicon (Si) and other low atomic numbers that are very important for coal-rock perception but difficult to detect with other analytical techniques. Its technical characteristics are very suitable for the needs of the coal industry. Research on coal-rock recognition based on LIBS technology has great theoretical value and practical significance. Through related research and technical research, the LIBS-CRR is expected to become an ideal solution for the application environment of various coal production links.

There have been many related studies on the application of LIBS in the coal industry in China and other countries, and certain scientific research results have been achieved in the field of coal quality testing.

Yin [46] designed a LIBS system device for coal quality measurements of C, H, Si, Na and other elements in coal powder, and the experimental results show that the experimental error of the system did not exceed 10%. At the same time, the minimum relative error of the regression analysis of the ash content in the pulverized coal is only 2.29%. Foreign Wallis *et al.* [47] conducted LIBS element analysis on lignite samples and obtained the detection limits for calcium (Ca), aluminum (Al), sodium (Na), iron (Fe), magnesium (Mg), silicon (Si) and other elements. Body *et al.* [48] developed a new type of LIBS instrument for coal quality analysis. The measurement accuracy for inorganic components, such as aluminum (Al), silicon (Si) and magnesium (Mg), was usually within a relative error of 10%. Ctvrtnickova *et al.* [49] showed the LIBS capability to characterize the components of coal ash. Gu [50] proposed a quantitative analysis method using partial least squares (PLS) and found that the quantitative accuracy was better than that of traditional methods. In addition, many other applied studies on data processing have also been reported [51]–[53].

Previous studies on LIBS dedicated to coal mines are theoretical studies in a laboratory environment, and there is no discussion of the in situ collection of LIBS spectra. Achieving in situ collection of LIBS spectra is an unavoidable practical problem in coal and rock identification. In addition,

the previous research has focused on the accuracy of element analysis, ignoring the real-time performance that is very important for coal and rock identification application scenarios. Research on simplifying the data structure of the spectrum is insufficient. Considering this gap in the current research, this paper will describe LIBS-CRR, which takes advantage of statistical principles, and the in situ sampling method is discussed in detail. To recognize the coal and rock, partial least-squares discriminant analysis (PLS-DA) is used to explore and verify the significant differences between coal and rock LIBS spectra and to simplify complex LIBS spectra to simultaneously build the simplified spectral model (SSM).

**II. MATERIAL AND METHODS**

**A. IN-SITU SAMPLING DESIGN**

A typical LIBS system (as shown in Fig. 1) generally consists of a PC, controller, pulse generator, laser, convex lens, spectrometer, intensified charge-coupled device (ICCD), etc. The laser was operated in external trigger mode and was triggered by a digital delay generator for synchronization with a repetition frequency. The Nd:YAG laser beam was focused on the sample through a convex lens at normal incidence. To avoid excessive ablation, the sample was mounted on a programmable translation electric sample stage. The laser was generally focused on a spot with a diameter of approximately 1 mm.

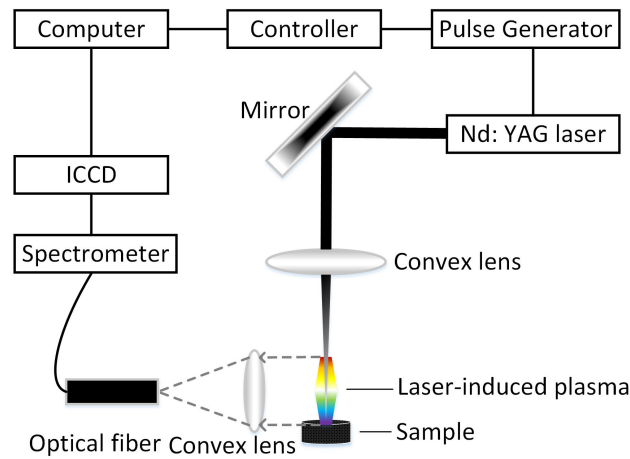
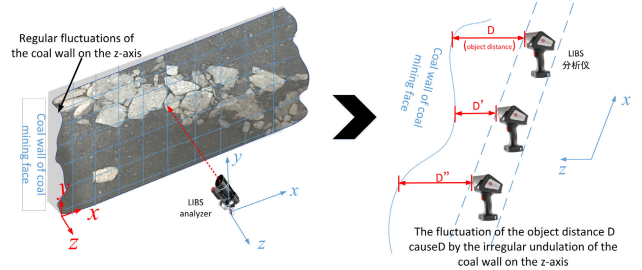


**FIGURE 1.** The typical LIBS system construction.

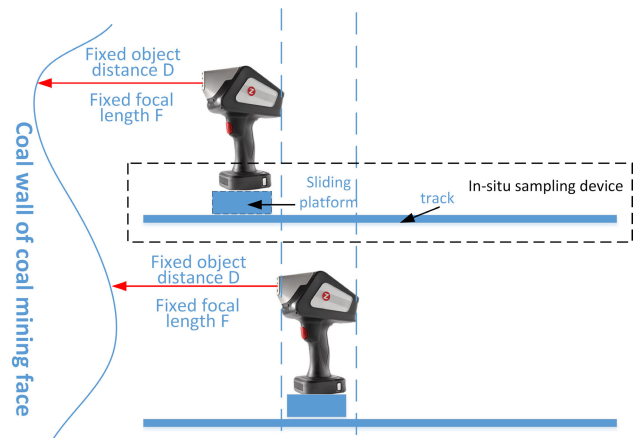
However, the application scenario of using coal-rock distribution information from the coal mining face to guide the operation of the shearer determines that the LIBS-CRR must have high real-time performance, so the spectra sampling process must be in situ sampled from the coal wall of the mining working face.

To overcome the challenge of in situ sampling, a handheld LIBS analyzer installed on a track parallel to the coal mining face was used to replace the traditional LIBS system. The handheld LIBS analyzer uses the track to distribute the sampling points on the (x-y) plane and uses the z-axis movement

induced by an automatically controlled sliding platform to offset the laser focus failure caused by the irregular undulation of the coal wall. Fig. 2 shows a schematic diagram of the in situ sampling of the mining working face.



**(a) In situ sampling of mining working face.**



**(b) Schematic diagram of the handheld LIBS analyzer, track and sliding platform.**

**FIGURE 2.** Schematic diagram of in situ sampling of the mining working face.

Laser pulses from a handheld LIBS analyzer (Z 200 C+, Sci-Aps) with a 1024-nm wavelength and maximum energy limited to 5.5 mJ/pulse are used to produce a laser-induced microplasma that meets the requirements of coal mine safety.

The LIBS analyzer is installed on a sliding platform. The sliding platform is driven by an electric motor using the back propagation network proportional-integral-derivative (BP-PID) control method to fix the object distance. Due to the fixed object distance, the laser can always be focused on the ideal position. Compared with zoom-type LIBS detection (such as telescope systems), the process is fully automated and the focusing speed is very fast. The focusing speed is approximately 80 ms, which is within the acceptable range for industrial application scenarios.

After the LIBS spectrum of the measured object is collected, the result of identification is obtained through the solution of the LIBS-CRR model. Finally, the shearer will operate according to the distribution of coal and rock.

Fig. 3 shows the LIBS-CRR model and the workflow of the LIBS-CRR system.

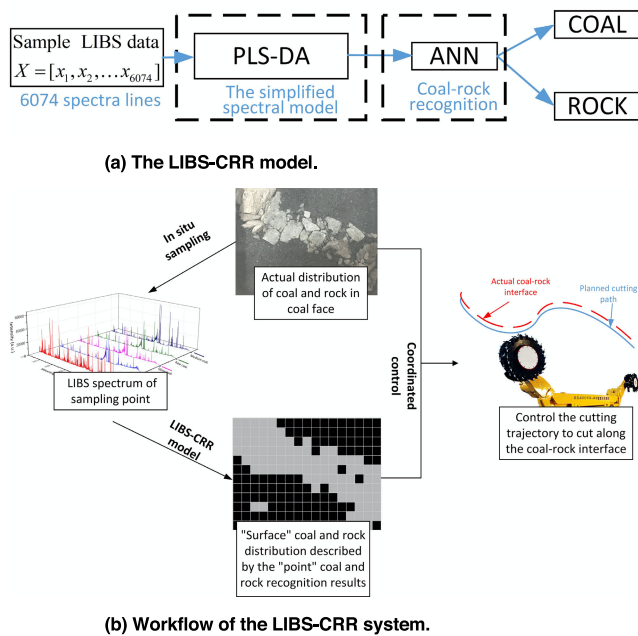


FIGURE 3. The overall structure of LIBS-CRR.

## B. SAMPLES

Four types of coal samples and two types of gangue samples were used for PLS-DA analysis to build the SSM and train the artificial neural network (ANN) classifier for coal-rock recognition. The samples were provided by the China Coal Technology Engineering Group.

The four types of coal were raw coal (RC), clean coal (CC), medium coal (MC), and slime coal (SC). Raw coal refers to coal that excludes only visible gangue without any other processing. After the coal was washed, the coal changed into high-quality coal suitable for special purposes; this is called clean coal. Medium coal refers to an intermediate product after the recovery of clean coal and the removal of gangue during coal separation and processing. These three types of coal were used to simulate different coal qualities. Slime coal generally refers to the semisolid matter formed by coal powder containing water, which is used to simulate the coal wetted by the water that is used to cool the shearer picks. The two types of rock were gangue (R1) and sandy mudstone (R2).

## III. RESULTS AND DISCUSSION

LIBS was used to test 10 group samples. Each group included one raw coal sample, one medium coal sample, one clean coal sample, one slime coal sample, one gangue sample and one sandy mudstone sample. A total of 60 samples were tested (sample library). Fig. 4 (a) shows some samples' spectra. Each sample's LIBS spectrum was acquired through 20 laser pulses at different sample points to reduce the data variations due to changes in the experimental conditions and contained 6074 spectral lines.

Due to the inherent plasma characteristics and mechanism, if the concentration of the measured substance is high,

self-absorption is usually unavoidable in LIBS measurements. The emission may be absorbed by the same kind of cold atoms in or around the plasma, resulting in a significant nonlinear relationship between the line intensity and element concentration. In addition, interelement interference caused by overlapping spectral lines and matrix effects is also common. Therefore, the intensity of a particular spectral line may come not only from a specific element but also from the number density of other elements in the plasma. In addition, many other factors and processes can change the measured characteristic line intensity, such as the spatial and temporal heterogeneity of the plasma. These twisting processes also change the line strengths, indicating that it is difficult to physically separate them. The only feasible way to achieve such separation is to apply data processing techniques to partially compensate for these deviations.

Due to the above deviation, the detection intensity of the characteristic line may not accurately reflect the element concentration, but it still contains basic information on the element concentration. With this in mind, a potential method is to extract the main concentration information from these characteristic lines and to further correct the model by considering the full range of spectra to compensate for the residuals. A paper on the measurement of carbon concentration in coal proposed a dominant factor model, in which the characteristic lines of the measured element or other elements were clearly extracted to explain the main part of the element concentration, and PLS was further applied to correct the model. The explicitly extracted expressions that dominate the final model results are called "dominant factors". The process of model building can be described as follows.

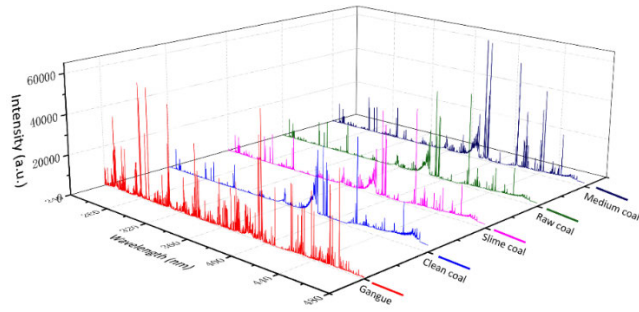
The first step is to extract the main relationship,  $f(I_i)$ , between the characteristic intensity  $I_i$  of the measured element  $i$  and elemental concentration  $C_i$ , which could be nonlinear under conditions in which the self-absorption effect cannot be neglected, as in Eq. 1.

$$C_i = f(I_i) \quad (1)$$

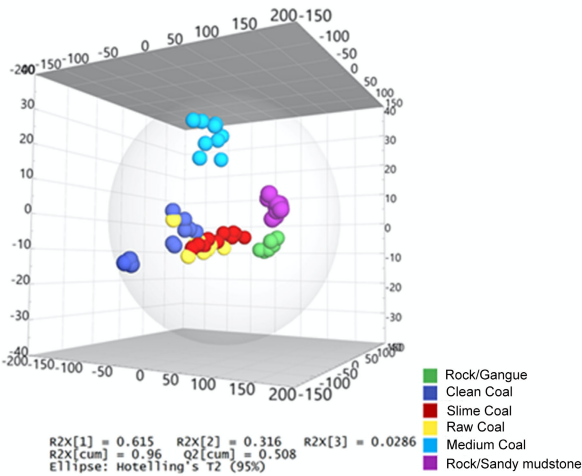
Interelement interference may be a major source of the difference, called the "residual", between the real element concentration and the value calculated with Eq. 1. However, the mechanism of interelement interference is complicated and remains unclear. In the present work, the second step is to model the interelement interference to further minimize the residuals using the best curve-fitting technology with nonlinear equations. After this process, the expression of the dominant factor is given in Eq. 2,

$$C_i' = f(I_i) + g(I_j) \quad (2)$$

where  $C_i'$  is the calculated elemental concentration considering the dominant factor of self-absorption and interelement interference,  $I_j$  is the intensity of the characteristic line affecting element  $j$ , and  $g(I_j)$  is the function describing interelement interference. After the dominant factors are extracted, the remaining differences may come from the imperfections of the dominant factors, other unknown deviation factors and



(a) Spectra of the coal and rock samples.



(b) The PLS-DA results of 60 samples.

FIGURE 4. The LIBS spectra of coal and rock and the corresponding data analysis.

even signal fluctuations, making it difficult to model these effects clearly. Considering that the entire spectrum contains useful information about the source of deviation, it is logical to use the full spectrum to further minimize the deviation. Therefore, the powerful multivariate PLS method is used to use the entire spectrum information to compensate for the residuals.

Please refer to Wang *et al.* for details on the approach [54], [55]. Eq. 3 shows the final expression of the model.

$$C_i'' = f(I_i) + g(I_j) + b_0 + b_1x_1 + \dots + b_nx_n \quad (3)$$

where  $C_i''$  represents the final calculated elemental concentration of the PLS model based on the dominant factor,  $x_1, x_2, \dots, x_n$  are the spectral intensities at different wavelengths, and  $b_0, b_1, b_2, \dots, b_n$  are the regression coefficients. Compared to the general PLS model, the PLS model based on the dominant factor should be more suitable for a wider matrix range because it binds the physical principles and uses the advantages of the multivariate PLS method to compensate for the residuals.

The dots in Fig. 4 (b) represent the scores of the samples on each principal component, and the distance between the points reflects the degree of similarity between the samples. Therefore, the spatial distribution of the PLS score map can

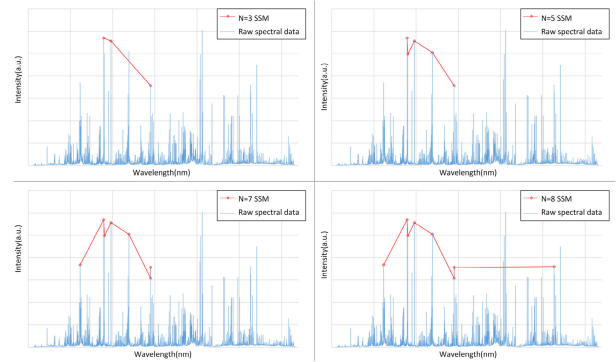


FIGURE 5. The SSM with different numbers of spectral lines.

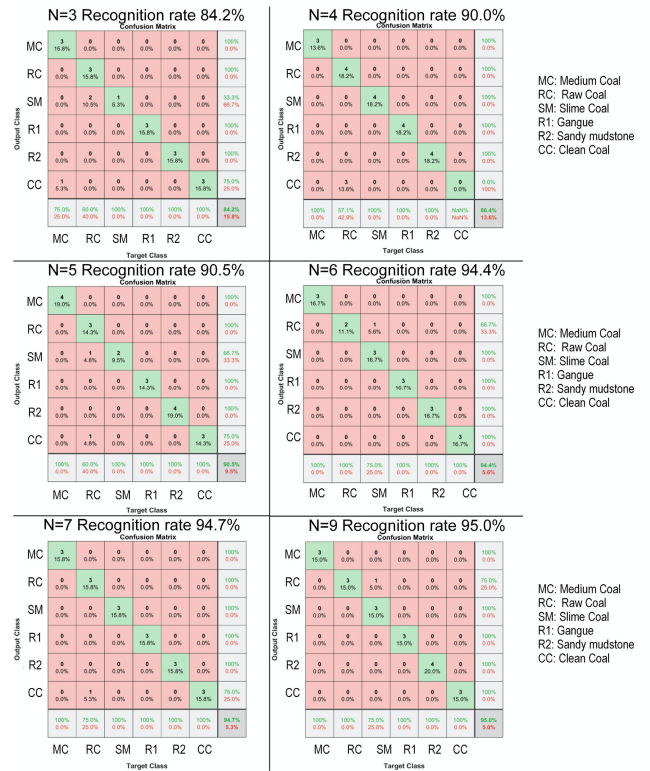


FIGURE 6. Experimental results of recognition by SSM with different N values.

intuitively reflect the similarities and differences between samples. The spatial distribution of coal and rock samples clearly reflects the differences between the groups, indicating that coal and rock have significant differences with respect to the statistical characteristics of LIBS spectroscopy; such characteristics can therefore be used to classify coal and rock.

The variations in the first three principal components were 0.615, 0.316 and 0.0286. The first three principal components interpret the original overall data up to 0.96.

This means that 3 principal components can be used to represent the original data, and general research uses the same approach. However, it is worth mentioning that each principal component was calculated from all the

**TABLE 1.** The top 15 wavelengths with the highest VIP values and their corresponding VIP values.

Var ID (wavelength)	VIP
288.09	6.04037
279.48	5.92436
334.94	5.53164
280.2	5.46063
309.39	5.36738
453.35	5.20912
334.88	5.10374
251.58	5.06804
453.59	4.96057
247.82	2.50742

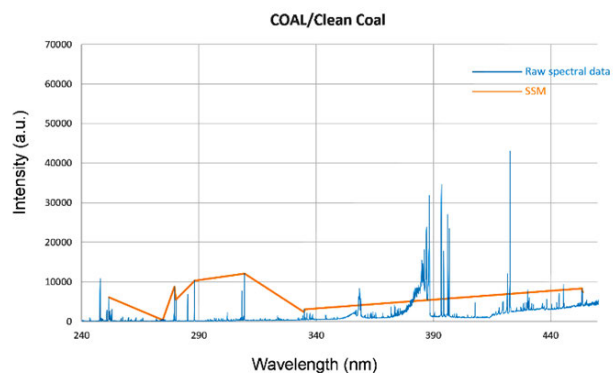
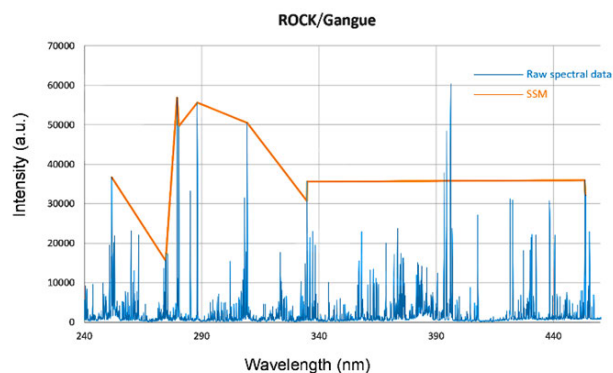


**FIGURE 7.** Comparison of the raw spectral data and the SSM data (N=10).

variable data of the original spectrum, and its expression contained all the spectral line data. The calculation process for statistical analysis and calculation of principal components was still relatively complicated, and engineering

Output Class	MC	RC	SM	R1	R2	CC	Accuracy
MC	3 14.3%	0 0.0%	0 0.0%	0 0.0%	0 0.0%	0 0.0%	100% 0.0%
RC	0 0.0%	2 9.5%	1 4.8%	0 0.0%	0 0.0%	0 0.0%	66.7% 33.3%
SM	0 0.0%	0 0.0%	4 19.0%	0 0.0%	0 0.0%	0 0.0%	100% 0.0%
R1	0 0.0%	0 0.0%	0 0.0%	3 14.3%	0 0.0%	0 0.0%	100% 0.0%
R2	0 0.0%	0 0.0%	0 0.0%	0 0.0%	4 19.0%	0 0.0%	100% 0.0%
CC	0 0.0%	0 0.0%	0 0.0%	0 0.0%	0 0.0%	4 19.0%	100% 0.0%
	100% 0.0%	100% 0.0%	80.0% 20.0%	100% 0.0%	100% 0.0%	100% 0.0%	95.2% 4.8%

(a) Recognition results for coal-rock (6 classifications).

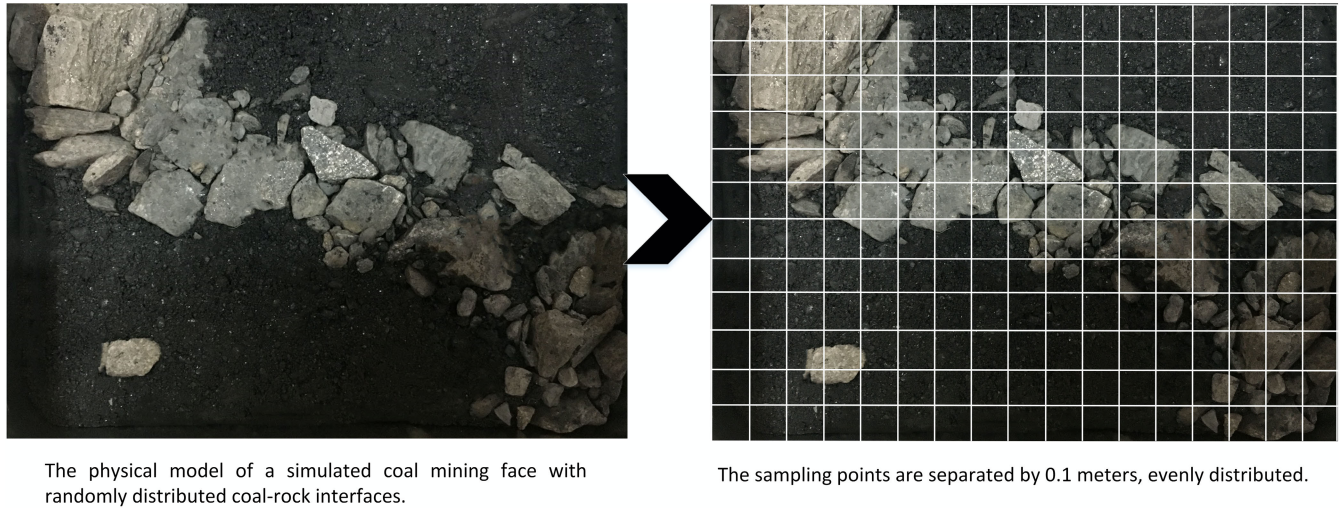
Output Class	coals	rocks	Accuracy
coals	13 65.0%	0 0.0%	100% 0.0%
rocks	0 0.0%	7 35.0%	100% 0.0%
	100% 0.0%	100% 0.0%	100% 0.0%

(b) Recognition results for coal-rock (2 classifications).

**FIGURE 8.** Results of the LIBS-based coal-rock recognition.

applications needed higher requirements for data processing chips and data storage space. Therefore, it was necessary and important to establish a SSM to optimize the LIBS-CRR method; this SSM contained a small amount of spectral line data.

The variable importance in projection (VIP) is a popular measurement tool in PLS-DA. The VIP quantifies the responses of each variable summed over all components and categorical responses, enabling the measurement of the global effect of each wavelength. The VIP values obtained in this article were calculated using SIMCA® (Sartorius Stedim Biotech) software. When the dependent variable is categorical data, the PLS-DA analysis method can not only find the principal components obtained from the linear combination of the variables but also analyze the VIP value. That is, the weight of the influence of each spectral line on the final coal and rock recognition result can be obtained.



The physical model of a simulated coal mining face with randomly distributed coal-rock interfaces.

The sampling points are separated by 0.1 meters, evenly distributed.

**FIGURE 9.** The random coal-rock interface of the specimen.

Dimension reduction and classification were the main purposes of the SSM. In this research, the SSM was built by the spectral lines according to the VIP value of the spectral line. Therefore, an appropriate number of feature components are selected to establish the SSM.

The number ( $N$ ) of spectral lines of a simple spectral model was the key issue. The number ( $N$ ) of spectral lines selected by the SSM increases from 3, and spectral lines are selected one by one according to the VIP value in Table 1, which is arranged from high to low.

Figure 5 shows the SSM with different numbers ( $N$ ) of spectral lines. The red line represents the simplified SSM spectrum of the sample spectrum.

Fig. 6 shows the effect of the ANN classifier trained for the SSM with different numbers of spectral lines on coal and rock recognition.

Through experiments, it was found that after  $N$  exceeded 9, the effect of improving the accuracy of coal and rock recognition was already very small, but the increase in  $N$  directly affected the complexity of the ANN classifier and the overall amount of calculation.

It is worth mentioning that when we classified and identified the coal and rock spectra, we considered not only the statistical significance but also the physical significance. In this study, considering that coal is a very complex substance that includes sulfides and oxides, we decided to use 10 characteristic wavelengths to construct the SSM while balancing the simplification and model accuracy considerations. Carbon is of obvious importance for the analysis of coal. In fact, because carbon atoms have a large number of peripheral electrons that are difficult to ionize, their spectral intensity is affected. This may be the reason why the VIP value of carbon is not very high. Therefore, even though the VIP value of the carbon line (247.82 nm) is not in the top ten (VIP=2.51), we decided to use it in the SSM. The selected 10 wavelengths

of SSM are listed in Table 1. Taking the spectra of a gangue sample and a clean coal sample as an example, the spectra of the 6074 wavelengths data were reduced to 10 wavelengths by SSM, as shown in Fig. 7.

By applying the SSM, the data volume of single sample spectra decreased from 6074 wavelengths to 10 wavelengths, representing 99.8% decrease with respect to the raw data.

After randomly selecting samples from the sample library as the training set to train the neural network algorithm, 20 samples were randomly selected from the remaining samples for recognition testing. The recognition results showed that one of the three raw coal samples was recognized as slime coal, and the remaining samples were correctly recognized. On the other hand, if the results were analyzed in the coal and rock category, all 13 coal samples and 7 rock samples were correctly recognized. Fig. 8 shows the corresponding results.

The coal-rock interface was random during the actual cutting process. Therefore, we made a physical model of a simulated coal mining face with randomly distributed coal-rock interfaces to verify the effectiveness of the LIBS-based CRR, as shown in Fig. 9. The model is 1.7 meters long and 1.2 meters wide. The LIBS data were tested by the in situ sampling method described in Fig. 2.

The sampling points were separated by 0.1 meters, and the recognition result of the sampling points was used as the recognition result of the square area where the sampling points were located.

A total of 204 sampling points were evenly distributed in the identification area, and the coal and rock distribution of the simulated coal mining face was described by these 204 squares. The coal and rock recognition results at the sampling points are shown in different colors. Black indicates that the recognition result of the sampling point was “coal”, and gray indicates that the recognition result of the sampling point was “rock”.

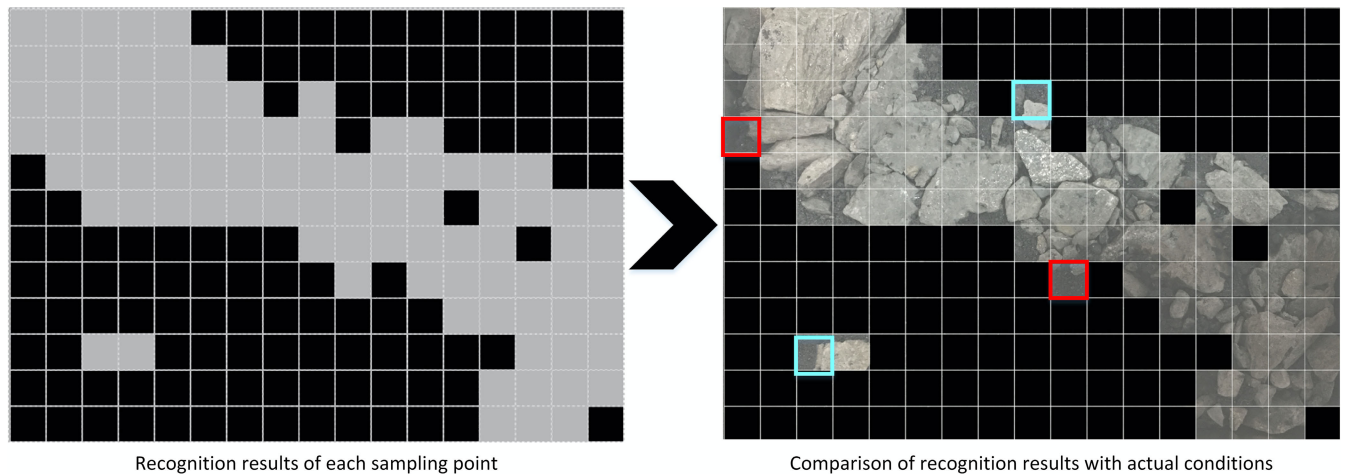


**FIGURE 10.** Recognition results.

The results of 204 test points are shown in Fig. 10. The red box in the figure marks the sampling points that were clearly recognized incorrectly. Because such sampling points were close to the coal-rock interface, the amount of gangue in the coal increased significantly, leading to a misjudgment. The blue box marks the sampling point for which the recognition result was uncertain. There were both coal and rock in the area, so the reason for determining it as rock may be that the sampling point did fall on the rock, or it may be that the sampling point fell on the coal but was misjudged as rock. Therefore, the number of sampling points for coal and rock recognition errors is 2-4, and the accuracy of sampling point recognition is between 98.03% and 99.01%. The recognition results of coal-rock recognition were close to those of the actual interface. The experimental results proved that the new CRR method presented in this paper is accurate and effective and has the inherent advantages of LIBS, including as fast, safe, and in situ measurement capabilities.

#### IV. CONCLUSION

In this research, a fast and accurate new idea for the coal-rock recognition in unmanned coal mining based on LIBS is presented and discussed in detail.

This method consists of three steps. First, LIBS spectra were obtained in situ, and emission spectra data were recorded. Then, PLS-DA was used to analyze the spectral data of all samples to construct the SSM. Finally, ANN was used to classify coal and rock based on the SSM.

The experimental results for the physical model of a simulated coal mining face with randomly distributed coal-rock interfaces prove the effectiveness of the method. The results showed that the accuracy of the classification model exceeded 97%. While ensuring the recognition accuracy, the amount of calculation data was reduced from 6074 wavelengths to 10 wavelengths, indicating that SSM is accurate and LIBS-CRR requires fewer calculations and less time than other methods.

The in situ collection of LIBS spectrum and LIBS-CRR real-time performance were all reasonably and effectively realized. The greatest key problem in applying LIBS technology to coal mine production sites for coal and rock identification will no longer be an obstacle. The results of this research provide a solid theoretical basis for practical applications.

Theoretically, the LIBS-CRR can be used to classify coal and rock effectively, quickly and accurately. The results of coal-rock recognition meet the expectations to provide an operational basis for unmanned coal mining equipment.

#### CONFLICTS OF INTERESTS

The authors have no conflicts of interest to declare that are relevant to the content of this article.

#### REFERENCES

- [1] S. Jiping, "Study on identified method of coal and rock interface based on image identification," *Coal Sci. Technol.*, vol. 39, no. 2, pp. 77–79, 2011.
- [2] C. Liu, J. Jiang, and W. Qu, "Research and design of excavation face remote reproduction and remote control systems," in *Advances in Energy and Environment Research*. Guangzhou, China: CRC Press, Aug. 2016, p. 323.
- [3] H. Wang and Q. Zhang, "Dynamic identification of coal-rock interface based on adaptive weight optimization and multi-sensor information fusion," *Inf. Fusion*, vol. 51, pp. 114–128, Nov. 2019.
- [4] W. Li, Y. Wang, B. Fu, and Y. Lin, "Coal and coal gangue separation based on computer vision," in *Proc. 5th Int. Conf. Frontier Comput. Sci. Technol.*, Aug. 2010, pp. 467–472.
- [5] X.-L. Zhang, R.-S. Jia, X.-M. Lu, Y.-J. Peng, and W.-D. Zhao, "Identification of blasting vibration and coal-rock fracturing microseismic signals," *Appl. Geophys.*, vol. 15, no. 2, pp. 280–289, Jun. 2018.
- [6] Y. F. Wang, Y. T. Xia, and X. C. Wang, "Application on overcomplete ICA with noise in coal and rock identification of fully mechanized mining," *J. China Coal Soc.*, vol. 36, no. S1, pp. 203–206, 2011.
- [7] Y. Liu, S. Dhakal, and B. Hao, "Coal and rock interface identification based on wavelet packet decomposition and fuzzy neural network," *J. Intell. Fuzzy Syst.*, vol. 38, no. 4, pp. 3949–3959, Apr. 2020.
- [8] L. Si, Z.-B. Wang, and G. Jiang, "Fusion recognition of shearer coal-rock cutting state based on improved RBF neural network and D-S evidence theory," *IEEE Access*, vol. 7, pp. 122106–122121, 2019.
- [9] F. Hu, M. Zhou, P. Yan, K. Bian, and R. Dai, "Multispectral imaging: A new solution for identification of coal and gangue," *IEEE Access*, vol. 7, pp. 169697–169704, 2019.



- [10] Z. Yang, Z. Wang, and M. Yan, "Performance analysis of natural  $\gamma$ -ray coal seam thickness sensor and its application in automatic adjustment of Shearer's arms," *J. Electr. Comput. Eng.*, vol. 2020, pp. 1–10, Aug. 2020.
- [11] L. Si, Z. Wang, Y. Liu, and C. Tan, "Online identification of shearer cutting state using infrared thermal images of cutting unit," *Appl. Sci.*, vol. 8, no. 10, p. 1772, Sep. 2018.
- [12] Z. Yan, Z. XinLei, J. WenBao, S. Qing, L. YongSheng, H. DaQian, and C. Da, "Online X-ray fluorescence (XRF) analysis of heavy metals in pulverized coal on a conveyor belt," *Appl. Spectrosc.*, vol. 70, no. 2, pp. 272–278, Feb. 2016.
- [13] M. Borsaru, B. Zhou, T. Aizawa, H. Karashima, and T. Hashimoto, "Automated lithology prediction from PGNA and other geophysical logs," *Appl. Radiat. Isot.*, vol. 64, no. 2, pp. 272–282, Feb. 2006.
- [14] M. Borsaru and Z. Jecny, "Application of PGNA for bulk coal samples in a  $4\pi$  geometry," *Appl. Radiat. Isot.*, vol. 54, no. 3, pp. 519–526, Mar. 2001.
- [15] M. Kaihara, T. Takahashi, T. Akazawa, T. Sato, and S. Takahashi, "Application of near infrared spectroscopy to rapid analysis of coals," *Spectrosc. Lett.*, vol. 35, no. 3, pp. 369–376, Jul. 2002.
- [16] M. Gaft, E. Dvir, H. Modiano, and U. Schone, "Laser induced breakdown spectroscopy machine for online ash analyses in coal," *Spectrochim. Acta B, At. Spectrosc.*, vol. 63, no. 10, pp. 1177–1182, Oct. 2008.
- [17] T. Zhang, C. Yan, J. Qi, H. Tang, and H. Li, "Classification and discrimination of coal ash by laser-induced breakdown spectroscopy (LIBS) coupled with advanced chemometric methods," *J. Anal. At. Spectrometry*, vol. 32, no. 10, pp. 1960–1965, 2017.
- [18] M. A. Badday, N. Bidin, Z. H. Rizvi, and R. Hosseinian, "Determination of environmental safety level with laser-induced breakdown spectroscopy technique," *Chem. Ecol.*, vol. 31, no. 4, pp. 379–387, May 2015.
- [19] D. Prochazka, M. Mazura, O. Samek, K. Rebrošová, P. Pořízka, J. Klus, P. Prochazková, J. Novotný, K. Novotný, and J. Kaiser, "Combination of laser-induced breakdown spectroscopy and Raman spectroscopy for multivariate classification of bacteria," *Spectrochim. Acta B, At. Spectrosc.*, vol. 139, pp. 6–12, Jan. 2018.
- [20] S. Manzoor, S. Moncayo, F. Navarro-Villoslada, J. A. Ayala, R. Izquierdo-Hornillos, F. J. M. de Villena, and J. O. Caceres, "Rapid identification and discrimination of bacterial strains by laser induced breakdown spectroscopy and neural networks," *Talanta*, vol. 121, pp. 65–70, Apr. 2014.
- [21] F. Ruan, T. Zhang, and H. Li, "Laser-induced breakdown spectroscopy in archeological science: A review of its application and future perspectives," *Appl. Spectrosc. Rev.*, vol. 54, no. 7, pp. 573–601, Aug. 2019.
- [22] S. Guirado, F. J. Fortes, and J. J. Laserna, "Elemental analysis of materials in an underwater archeological shipwreck using a novel remote laser-induced breakdown spectroscopy system," *Talanta*, vol. 137, pp. 182–188, May 2015.
- [23] A. K. Myakalwar, S. Sreedhar, I. Barman, N. C. Dingari, S. V. Rao, P. P. Kiran, S. P. Tewari, and G. M. Kumar, "Laser-induced breakdown spectroscopy-based investigation and classification of pharmaceutical tablets using multivariate chemometric analysis," *Talanta*, vol. 87, pp. 53–59, Dec. 2011.
- [24] P. K. Tiwari, N. K. Rai, R. Kumar, C. G. Parigger, and A. K. Rai, "Atomic and molecular laser-induced breakdown spectroscopy of selected pharmaceuticals," *Atoms*, vol. 7, no. 3, p. 71, Jul. 2019.
- [25] S. Qiao, Y. Ding, D. Tian, L. Yao, and G. Yang, "A review of laser-induced breakdown spectroscopy for analysis of geological materials," *Appl. Spectrosc. Rev.*, vol. 50, no. 1, pp. 1–26, Jan. 2015.
- [26] G. S. Senesi, "Laser-induced breakdown spectroscopy (LIBS) applied to terrestrial and extraterrestrial analogue geomaterials with emphasis to minerals and rocks," *Earth-Sci. Rev.*, vol. 139, pp. 231–267, Dec. 2014.
- [27] B. Sallé, J.-L. Lacour, E. Vors, P. Fichet, S. Maurice, D. A. Cremers, and R. C. Wiens, "Laser-induced breakdown spectroscopy for Mars surface analysis: Capabilities at stand-off distances and detection of chlorine and sulfur elements," *Spectrochim. Acta B, At. Spectrosc.*, vol. 59, no. 9, pp. 1413–1422, Sep. 2004.
- [28] D. A. Cremers, "Space applications of LIBS," in *Laser-Induced Breakdown Spectroscopy*. Berlin, Germany: Springer, 2014, pp. 257–291.
- [29] J. L. Gottfried, F. C. De Lucia, C. A. Munson, and A. W. Miziolek, "Double-pulse stand-off laser-induced breakdown spectroscopy for versatile hazardous materials detection," *Spectrochim. Acta B, At. Spectrosc.*, vol. 62, no. 12, pp. 1405–1411, Dec. 2007.
- [30] A. Sarkar, R. K. Mishra, C. P. Kaushik, P. K. Wattal, D. Alamelu, and S. K. Aggarwal, "Analysis of barium borosilicate glass matrix for uranium determination by using ns-IR-LIBS in air and Ar atmosphere," *Radiochim. Acta*, vol. 102, no. 9, pp. 805–812, Sep. 2014.
- [31] M. Singh, V. Karki, R. K. Mishra, A. Kumar, C. P. Kaushik, X. Mao, R. E. Russo, and A. Sarkar, "Analytical spectral dependent partial least squares regression: A study of nuclear waste glass from thorium based fuel using LIBS," *J. Anal. At. Spectrometry*, vol. 30, no. 12, pp. 2507–2515, 2015.
- [32] J. Savovic, M. Momcilovic, S. Zivkovic, A. Stancalie, M. Trtica, and M. Kuzmanovic, "LIBS analysis of geomaterials: Comparative study of basalt plasma induced by TEA CO<sub>2</sub> and Nd:YAG laser in air at atmospheric pressure," *J. Chem.*, vol. 2017, pp. 1–9, Jul. 2017.
- [33] R. R. Hark and R. S. Harmon, "Geochemical fin-gerprinting using LIBS," in *Laser-Induced Break-Down Spectroscopy*. Berlin, Germany: Springer, 2014, pp. 309–348.
- [34] L. Zhang, S. Ji, S. Gu, X. Huang, J. E. Palmer, W. Giewont, F. F. Wang, and L. M. Tolbert, "Design considerations for high-voltage insulated gate drive power supply for 10-kV SiC MOSFET applied in medium-voltage converter," *IEEE Trans. Ind. Electron.*, vol. 68, no. 7, pp. 5712–5724, Jul. 2021.
- [35] S. Sheta, M. S. Afgan, Z. Hou, S.-C. Yao, L. Zhang, Z. Li, and Z. Wang, "Coal analysis by laser-induced breakdown spectroscopy: A tutorial review," *J. Anal. At. Spectrometry*, vol. 34, no. 6, pp. 1047–1082, 2019.
- [36] J.-S. Wang, Y.-Z. Lu, W.-L. Li, D.-P. Qiao, and Y. Tang, "Laser-induced breakdown spectroscopic technique for analyzing rock and coal samples," *Metall. Anal.*, vol. 29, no. 1, pp. 30–34, 2009.
- [37] N. B. Fietz and T. Bartnitzki, "Latest developments in LIBS for distinction of coal and waste rock in explosive areas," *Mining Rep.*, vol. 152, no. 5, pp. 1–9, 2016.
- [38] J. Zeng, H. Xu, G. Gong, C. Xu, C. Tian, T. Lu, and R. Jiang, "Hackem-LIBS: An heterogeneous stacking ensemble model for laser-induced breakdown spectroscopy elemental quantitative analysis," *IEEE Access*, vol. 8, pp. 136141–136150, 2020.
- [39] D. A. Cremers and L. J. Radziemski, *Handbook of Laser-Induced Breakdown Spectroscopy*. Hoboken, NJ, USA: Wiley, 2013.
- [40] Z. Hou, Z. Wang, T. Yuan, J. Liu, Z. Li, and W. Ni, "A hybrid quantification model and its application for coal analysis using laser induced breakdown spectroscopy," *J. Anal. At. Spectrometry*, vol. 31, no. 3, pp. 722–736, 2016.
- [41] D. W. Hahn and N. J. A. S. Omenetto, "Laser-induced breakdown spectroscopy (LIBS)—Part I: Review of basic diagnostics and plasma-particle interactions: Still-challenging issues within the analytical plasma community," *Appl. Spectrosc.*, vol. 64, no. 12, pp. 335A–366A, 2010.
- [42] Y. He, "Application of laser to research of gas explosion mechanism," *Xi'an Univ. Sci. Technol. J.*, vol. 22, no. 4, pp. 482–485, 2002.
- [43] V. K. Unnikrishnan, K. S. Choudhari, S. D. Kulkarni, R. Nayak, V. B. Kartha, and C. Santhosh, "Analytical predictive capabilities of laser induced breakdown spectroscopy (LIBS) with principal component analysis (PCA) for plastic classification," *RSC Adv.*, vol. 3, no. 48, pp. 25872–25880, 2013.
- [44] J. Feng, Z. Wang, L. West, Z. Li, and W. Ni, "A PLS model based on dominant factor for coal analysis using laser-induced breakdown spectroscopy," *Anal. Bioanal. Chem.*, vol. 400, no. 10, pp. 3261–3271, Jul. 2011.
- [45] J. Álvarez, M. Velásquez, A. K. Myakalwar, C. Sandoval, R. Fuentes, R. Castillo, D. Sbarbaro, and J. Yáñez, "Determination of copper-based mineral species by laser induced breakdown spectroscopy and chemometric methods," *J. Anal. At. Spectrometry*, vol. 34, no. 12, pp. 2459–2468, 2019.
- [46] W. Yin, L. Zhang, L. Dong, W. Ma, and S. Jia, "Design of a laser-induced breakdown spectroscopy system for on-line quality analysis of pulverized coal in power plants," *Appl. Spectrosc.*, vol. 63, no. 8, pp. 865–872, Aug. 2009.
- [47] F. J. Wallis, B. L. Chadwick, and R. J. S. Morrison, "Analysis of lignite using laser-induced breakdown spectroscopy," *Appl. Spectrosc.*, vol. 54, no. 8, pp. 1231–1235, Aug. 2000.
- [48] D. Body and B. L. Chadwick, "Optimization of the spectral data processing in a LIBS simultaneous elemental analysis system," *Spectrochim. Acta B, At. Spectrosc.*, vol. 56, no. 6, pp. 725–736, Jun. 2001.
- [49] T. Cvrtnickova, M.-P. Mateo, A. Yáñez, and G. Nicolas, "Characterization of coal fly ash components by laser-induced breakdown spectroscopy," *Spectrochim. Acta B, At. Spectrosc.*, vol. 64, no. 10, pp. 1093–1097, Oct. 2009.
- [50] Y.-H. Gu, Y. Li, Y. Tian, and Y. Lu, "Study on the multivariate quantitative analysis method for steel alloy elements using LIBS," *Spectrosc. Spectral Anal.*, vol. 34, no. 8, pp. 2244–2249, 2014.
- [51] R. Wang, Q. Sun, P. Tu, J. Xiao, Y. Gui, and P. Wang, "Reduced-order aggregate model for large-scale converters with inhomogeneous initial conditions in DC microgrids," *IEEE Trans. Energy Convers.*, vol. 36, no. 3, pp. 2473–2484, Sep. 2021.

- [52] Y. Li, D. W. Gao, W. Gao, H. Zhang, and J. Zhou, "A distributed double-Newton descent algorithm for cooperative energy management of multiple energy bodies in energy internet," *IEEE Trans. Ind. Informat.*, vol. 17, no. 9, pp. 5993–6003, Sep. 2021.
- [53] Y. Li, W. Gao, W. Yan, S. Huang, R. Wang, V. Gevorgian, and D. Gao, "Data-driven optimal control strategy for virtual synchronous generator via deep reinforcement learning approach," *J. Mod. Power Syst. Clean Energy*, vol. 9, no. 4, pp. 919–929, 2021.
- [54] Z. Wang, J. Feng, L. Li, W. Ni, and Z. Li, "A mul-tivariate model based on dominant factor for laser-induced breakdown spectroscopy measurements," *J. Anal. At. Spectrometry*, vol. 26, no. 11, pp. 2289–2299, 2011.
- [55] Z. Wang, J. Feng, L. Li, W. Ni, and Z. Li, "A non-linearized PLS model based on multivariate domi-nant factor for laser-induced breakdown spectros-copy measurements," *J. Anal. At. Spectrometry*, vol. 26, no. 11, pp. 2175–2182, 2011.



**YIMIN LUO** was born in Huaian, China, in 1996. He received the master's degree from the China Coal Research Institute, in 2021. He is currently pursuing the Ph.D. degree with Shanghai Jiao Tong University, Shanghai, China.

His current research interests include distributed fiber optic sensing, control algorithms, and intelligent industrial equipment.



**CONG LIU** was born in Jiangsu, China, in 1988. He received the Ph.D. degree in electrical engineering from Shanghai Jiao Tong University, China, in 2020.

He currently works at China Coal Technology and Engineering Group Shanghai Company Ltd. His current research interests include intelligent industrial equipment, laser technologies, inertial navigation, and control algorithms.



**QIZHI ZHANG** was born in Anhui, China, in 1992. He received the master's degree from the China Coal Research Institute, in 2017. He is currently working at China Coal Technology Engineering Group Shanghai Company Ltd.

His current research interest includes shearer electrical control systems.

...